

Influence of Size and Number of Nanocrystals on Shear Band Formation in Amorphous Alloys

Junyoung Park, Yoji Shibutani, Masato Wakeda* and Shigenobu Ogata

Department of Mechanical Engineering, Osaka University, Suita 565-0871, Japan

In this study, binary (copper and zirconium) amorphous metals with embedded nanosized crystal structures are subjected to uniaxial tension using molecular dynamics simulations to reveal the mechanism of shear band structure formation. The number and the size of the nanocrystals are chosen as the study parameters. The number of nanocrystals affects the stress-strain curve and shear band formation while the size of the nanocrystals does not significantly affect the results. As reported in the experimental work published so far, under tension coalescent voids are found in the shear bands or at the interface between crystalline and amorphous materials. The simulation results show that the number of shear bands under compressive loading is much larger than that under tensile loading. We also found that, even under compressive loading, the shear bands started from regions with enough free volume. [doi:10.2320/matertrans.48.1001]

(Received January 11, 2007; Accepted February 22, 2007; Published April 25, 2007)

Keywords: amorphous alloy, shear band, nanocrystals, molecular dynamics, atomic strain, deformation participation ratio

1. Introduction

Since the first synthesis of a system with an amorphous phase by the rapid solidification technique, a great number of amorphous alloys have been produced.¹⁾ The development of alloys capable of forming bulk amorphous structures makes it possible to conduct mechanical deformation testing under a much wider range of loading conditions than was possible with earlier glass-forming alloys which could only be produced as thin ribbons.²⁾ Unlike crystalline materials, metallic glasses exhibit a remarkably high elastic modulus and strength on mechanical deformation. Although their mechanical behaviors have been extensively studied, the precise nature of the deformation mechanism in these amorphous metals still remains unclear.

The deformation behavior of an amorphous material is usually classified as an inhomogeneous or homogeneous deformation. It is well known from earlier work that its plastic deformation is concentrated into a narrow region called a shear band, except at temperatures sufficiently high to allow homogeneous deformation.³⁾ The resulting deformation depends on the loading conditions: unstable and abrupt failure of one or more shear bands occurs when the amorphous material is subjected to uniaxial tensile loading, whereas uniaxial compressive loading or bending results in multiple shear bands showing apparently elastic-perfect plastic deformation behavior.⁵⁻¹²⁾

It is important to understand the mechanism of shear band formation since the formation of localized shear bands is directly related to the phenomenon of high fragility, which is the typical characteristic of the deformation behaviors of amorphous materials. It is well known that the localized shear band is associated with local viscosity.⁴⁻⁶⁾ There are two prominent theories that remain controversial: the first is the theory of free volume in which the density of amorphous material decreases and the second suggests that local adiabatic heating beyond the glass transition temperature is the reason for the increase in viscosity. In both cases, a

change of viscosity drives the inhomogeneous deformation.⁴⁻⁶⁾

In order to avoid fragility, it is necessary to promote the formation of multiple shear bands.⁷⁻¹²⁾ Some research has reported that the presence of crystalline phases in metallic glasses in amounts up to 35% enhanced ductility or plastic strain, because the crystalline phases can promote multiple shear bands.⁷⁻⁹⁾ To improve the ductility, amorphous composite materials containing the second phases such as nanocrystals, ceramics particle, ductile metals and so on, have also been investigated up to date.¹⁰⁾ A decrease of yield stress and a reduction in the degree of deformation localization have been reported in these studies. Various aspects of amorphous composite materials have been studied previously. The yield strength of the composite is slightly lower than that of the monolithic amorphous material.^{7,11)} In tension tests, coalescent nanovoids are often observed along individual shear bands and at the interface between nanocrystalline and amorphous materials, while such nanovoids are rarely observed in compression tests.^{7,12)} Similarly, the nanocrystals observed in the earlier studies were seen only near shear bands.¹¹⁾ Conversely, there were no crystals found in the shear bands themselves. The crystal structure can hinder, deflect, and bifurcate the propagation of shear bands, resulting in multiple shear bands.⁹⁾

In this work, we explore the connection between the size or the number of crystals and the formation of shear bands. This choice is motivated by a number of recent publications investigating strain localization using molecular dynamics simulations.¹³⁻¹⁶⁾ These studies found that the mechanism of shear band formation was related to the roles of quasi-crystal-like short range order and the mass density of pure amorphous materials rather than the specimen including nanocrystal structures. Ironically, the shear bands terminate within or propagate through the nanocrystals. This means that while nanocrystalline material enhances the generation of shear bands, it also prevents the propagation of shear bands. It is thought that this dual nature is the reason why amorphous composite materials or amorphous materials containing nanocrystals are more ductile.

*Graduate Student, Osaka University

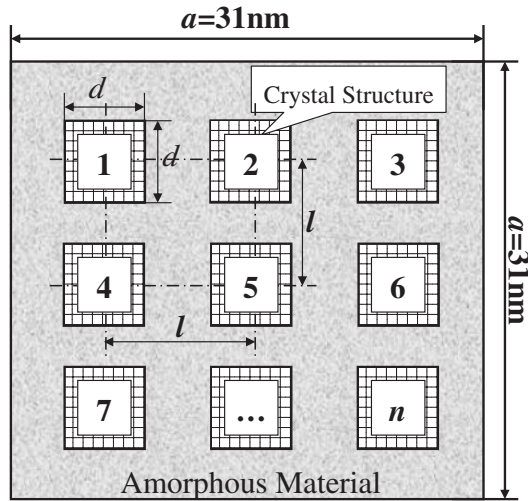


Fig. 1 Schematic of composite models where a is about 31 nm, d varies from 0.00 nm (pure amorphous materials) to 9.654 nm (the biggest crystal) and n (the number of crystals) varies from 0 to 81. The model is subject to compressive and tensile loading along the lateral direction.

2. Computational Model

We chose pure amorphous $\text{Cu}_{57}\text{Zr}_{43}$ system containing about 100,000 atoms as a representative model (Model 1). The detail computational process of constructing the amorphous state is given in reference.¹⁷⁾ The fully relaxed model has an approximate size of 31 nm \times 31 nm \times 17 nm. To easily understand the formation of shear bands during the deformation process, we employed 2-D molecular dynamics using a modified Lennard-Jones potential which is fitted for the amorphous $\text{Cu}_{57}\text{Zr}_{43}$ system,^{18,19)} in plane stress condition. This condition means that the z -coordinate of each atom is fixed in the 3-dimensional model. We choose the 3-dimensional model to measure the atomic strain using an already existing program.²⁰⁾ To the best of our knowledge, so far it is impossible to make multiple shear bands in tension or compression tests of a full 3-dimensional model with periodic boundary conditions, except for samples that have nano-order in thickness but, no periodic boundary conditions.¹⁵⁾ There are two reasons that, we suppose, are responsible for this difficulty: the degrees of freedom and the width of the shear bands. The shear band is a kind of strain localization, *i.e.* an unstable region. In a 3-D simulation, each atom can easily find a position where there is a local minimum in the energy corresponding to a stable state. Consequently, if we restrict a dimension in a 3-D simulation, it is easy to generate an unstable region such as a shear band while the full 3-D model is too homogeneous to generate such instabilities. The other reason is the limitation of the model size and the corresponding width of the shear band. The model we used in the paper might be too small to represent multiple shear bands in a 3-D simulation.

To investigate the size effect, we used the same models but with embedded artificial perfect crystal structures sized about 1 nm \times 1 nm (Model 2), 3 \times 3 nm (Model 3), and 9 nm \times 9 nm (Model 4), as shown in Fig. 1. The embedded crystal is Zr_2Cu having a perfect C11b structure as found in experiments on the binary system.²¹⁾ The measured Young's

Table 1 The size (d) and number (n) of the crystals embedded in each model. The volume fractions of crystals of models 4, 5, and 6 are identical. Model 1 is a pure amorphous sample.

n	d			
	0 nm	1 nm	3 nm	9 nm
0	Model 1			
1		Model 2	Model 3	Model 4
9			Model 5	
81		Model 6		

modulus of this crystal using molecular dynamics is 1.22 GPa, almost equal to that of the pure amorphous model. Before being embedded, the crystal model is also fully relaxed with periodic boundary conditions. In order to obtain the influence of the number of crystals on the amorphous materials, we varied the number from 0, corresponding to the pure amorphous structure, to 81 of the smallest sized crystals (Model 6). The details of the models used in this paper are summarized in Table 1. The volume fractions of crystals to amorphous materials are equal to 0.12% (Model 2), 1.1% (Model 3) and 9.5% (Model 4~6).

As the first step in a calculation, two models, one with the fully relaxed amorphous structure, and the other with the C11b crystal structure are prepared. Next, a hole with the same size of crystal is created in the amorphous materials and the crystals are embedded in the amorphous structure. Then, the mixed structure is fully relaxed for 100 ps, again. To make shear bands, the models are subject to uniaxial tension and uniaxial compression. The pressure is kept constant by changing the size of the whole model.

The atomic strain for each atom is measured using the definition suggested by Mott and Argon.²²⁾ Then, the deviatoric distortion is calculated using the measured atomic strain.²⁰⁾ In order to represent the deviatoric distortion, we use the octahedral strain expressed as follows:

$$\gamma_{oct} = \sqrt{\frac{1}{3} \text{Tr} \left(\varepsilon_{ij} - \frac{1}{3} \varepsilon_V \delta_{ij} \right)^2}, \quad (1)$$

where ε_V is the volumetric strain. This definition and more detail concerning it can be found in reference.²²⁾ In order to quantify the degree of strain localization, *i.e.* the amount of the shear band, a quantity called the deformation participation ratio (DPR), introduced by Shi and Falk, is utilized.¹⁵⁾ The definition of DPR is the fraction of atoms that have an atomic deviatoric shear strain larger than that of the whole system. In the case of strain localization, it should become small.

3. Results and Discussions

Uniaxial compressive and tensile loadings are applied to all models, until the strain reaches a value of 0.25 or -0.25 . Figure 2 shows stress-strain curves for the models with different sizes of crystal. During deformation, all curves reach a maximum then suddenly drop. The sudden drops are caused by the formation of a shear band. It has already been found that the cooling rate of samples and the deformation strain rate also affect to the maximum stress and the overall curve shape.¹⁵⁾ In the region of compression in Fig. 2, all

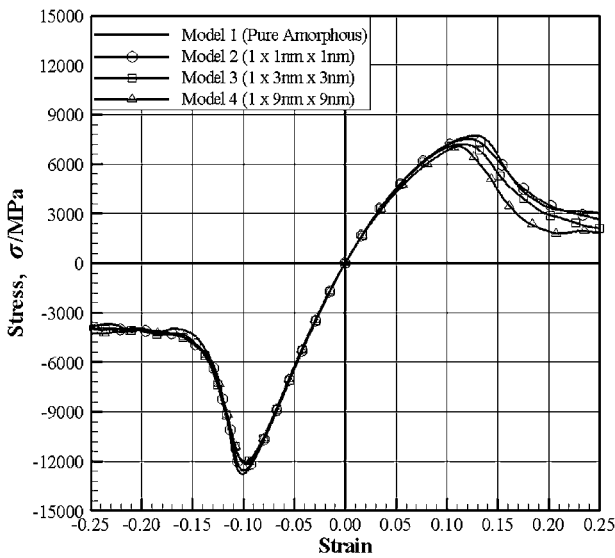


Fig. 2 Stress-strain curves for the models with different sizes of crystals.

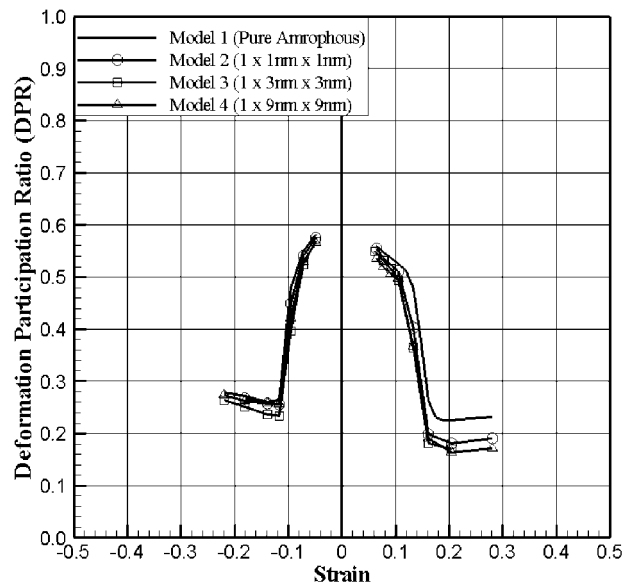


Fig. 4 Curve of DPR. vs. Strain. The size of the crystals has no effect on DPR except for model 1 under tension loading.

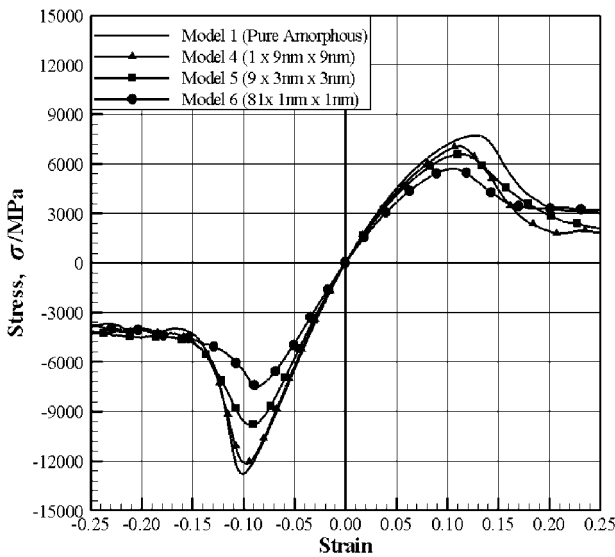


Fig. 3 Stress-strain curves for the models with different number of crystals. Models 1 and 4 in this figure are copies of model 1 and 4 in Figure 2.

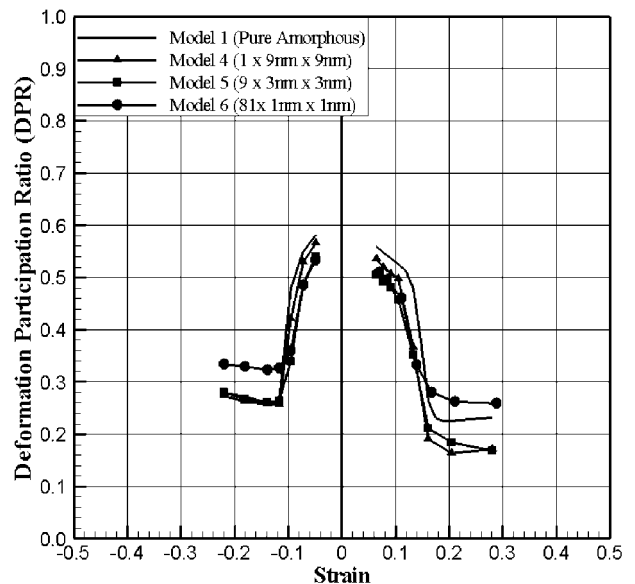


Fig. 5 Curve of DPR. vs. Strain. Model 6 with 81 crystals has a small DPR which means less localized deformation.

models exhibit an almost identical curve shape. The gradient of curve, which is the elastic modulus, the maximum stress, the corresponding strain and even the flow stress after the shear band formation look identical. This means that, under uniaxial compressive loading, the size of the crystals under uniaxial compressive loading does not significantly affect shear band formation. In the region of tensile loading, the maximum stress and the corresponding strain are slightly reduced. However, the amount of decrease is relatively small, compared with the case of the number of crystals discussed later. Consequently, the effect of crystal size is negligible for both tests.

However, Fig. 3 shows that the number of crystals embedded in the amorphous materials has a dramatic effect on the stress-strain curve. This is the reason why many researches are focused on the multi-nanocrystals. In the compression region, the maximum stress drops sharply as the

number of crystals increases. The drop of the maximum stress is necessary since shear bands are normally generated near or at the crystal, *i.e.* multi-crystals play a role as multi-sources for shear band formation. More details of the onset of shear band formation will be presented later. In Fig. 3, the strain corresponding to the maximum stress moves slightly to lower strain values; it originates in the lower elastic modulus of systems containing many crystals. However, the value flow stress remains almost constant, even if the number of crystals is changed. Nevertheless, the strain state of shear band could be different in each case.

Figure 4 depicts values of the DPR at given strains for different sizes of crystals. In compression tests, all curves suddenly drop around 0.1, corresponding to the maximum stress point of the stress-strain curve. All curves in Fig. 4

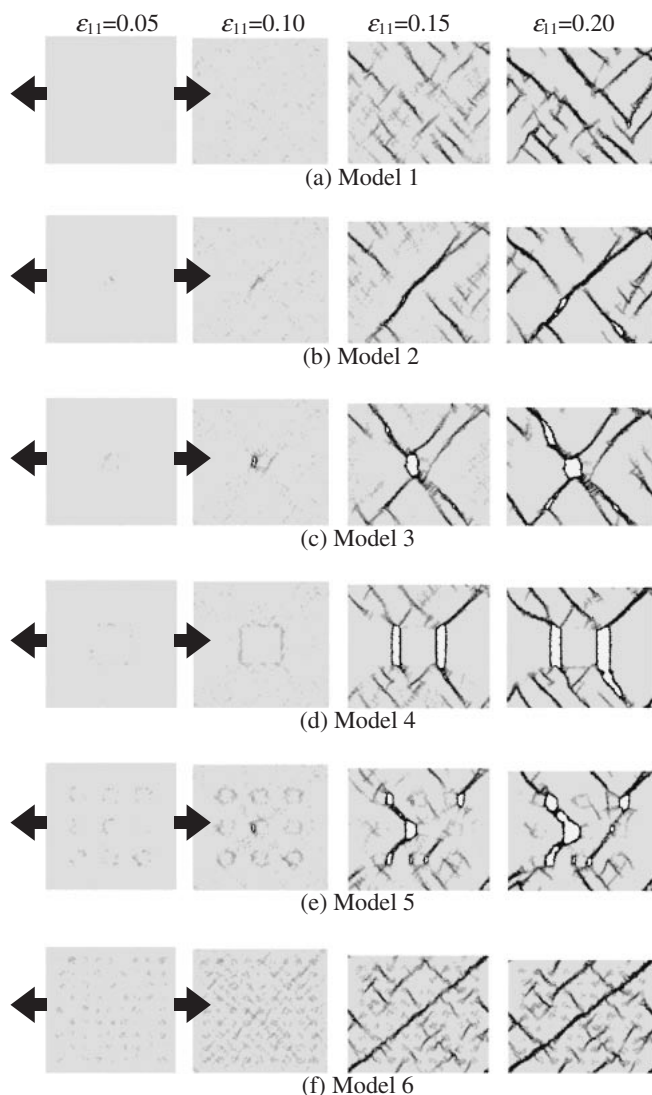


Fig. 6 Shear bands represented by the deviatoric shear strain of uniaxial tension for each model, from left to right with $\epsilon_{11} = 0.05, 0.10, 0.15$ and 0.20 . Atoms are colored according to the value of the atomic deviatoric shear strain. Black represents a strain greater than 1.0 while white represents 0.0 strain.

show almost identical trends, even after the drop. As before, this also means there is no noticeable effect of the crystal size. For the tension tests, all curves except model 1, which corresponds to pure amorphous material, fall mostly onto a single curve. Like the compression tests, the tension tests also indicate there is no relationship between the size of the crystals and shear band formation. Figure 4 also shows a good agreement with the experimental study in compression and tension tests, where the multiple shear bands corresponding to relatively high DPR are generated in compression tests, while just a few shear bands, corresponding to low DPR, are found in tension tests.⁷⁾ However, model 1 in the compression test is an exception. Although the DPR of model 1 in the compression test is still smaller than that in tension test, the difference between compression and tension is relatively small.

The DPR of models in the simulation is repeatable even for models with different initial atomic configurations. However, if there is even a very tiny crystal present, as for instance, in

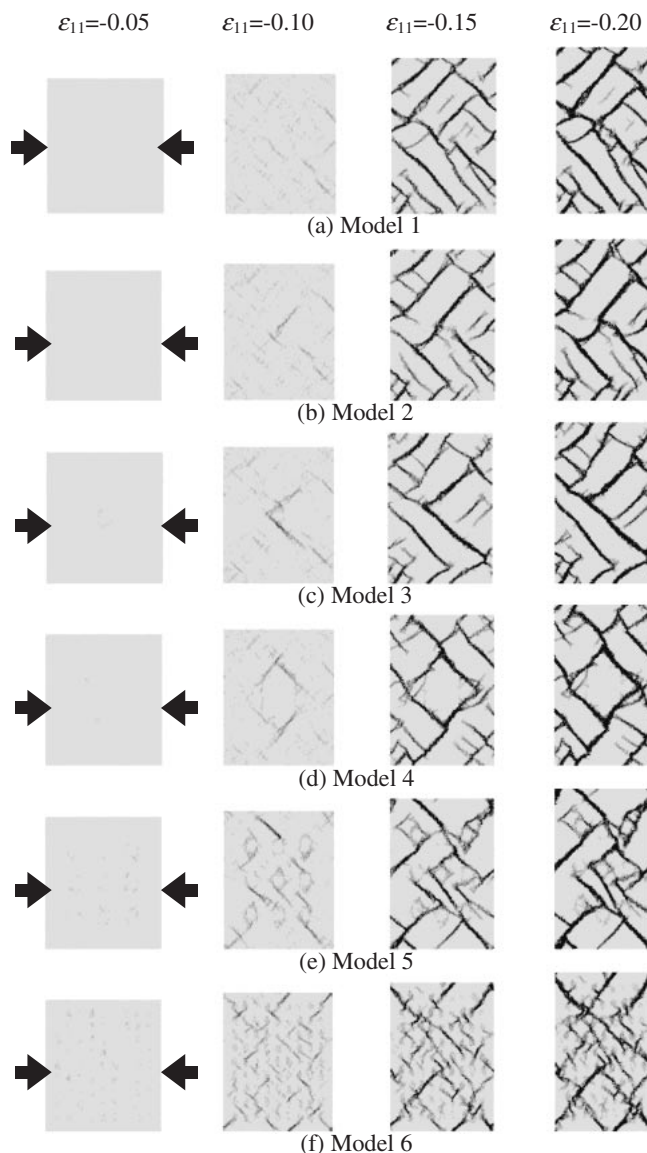


Fig. 7 Shear bands represented by the deviatoric shear strain of uniaxial compression for each model from left to right with $\epsilon_{11} = -0.05, -0.10, -0.15$ and -0.20 . Atoms are colored according to the value of the atomic deviatoric shear strain. Black represents a strain greater than 1.0 while white represents 0.0 strain.

model 2, which has a single 1 nm-sized crystal, it produces a totally different value on the DPR curve. Note the fraction of nanocrystal in this case is negligible (about 0.12%). One of the reasons we harbor suspicions about the results from model 1 is that in this computer simulation, this model has a structure that is too homogeneous, to a degree impossible to obtain in experiments. It seems that, due to its homogenous structure, model 1 has a relatively large DPR and produces more shear bands than expected, even under the tensile loading.

Unlike the effect of crystal size, Fig. 3 clearly shows that the shape of the stress-strain curve depends on the number of crystals. The maximum stress is inversely proportional to the number of crystals. However, with respect to the DPR values shown in Fig. 5, the trend is slightly different. Here, models 1, 4, and 5 have no noticeable differences for the both loading conditions. Only model 6 with 81 crystals has a greater DPR

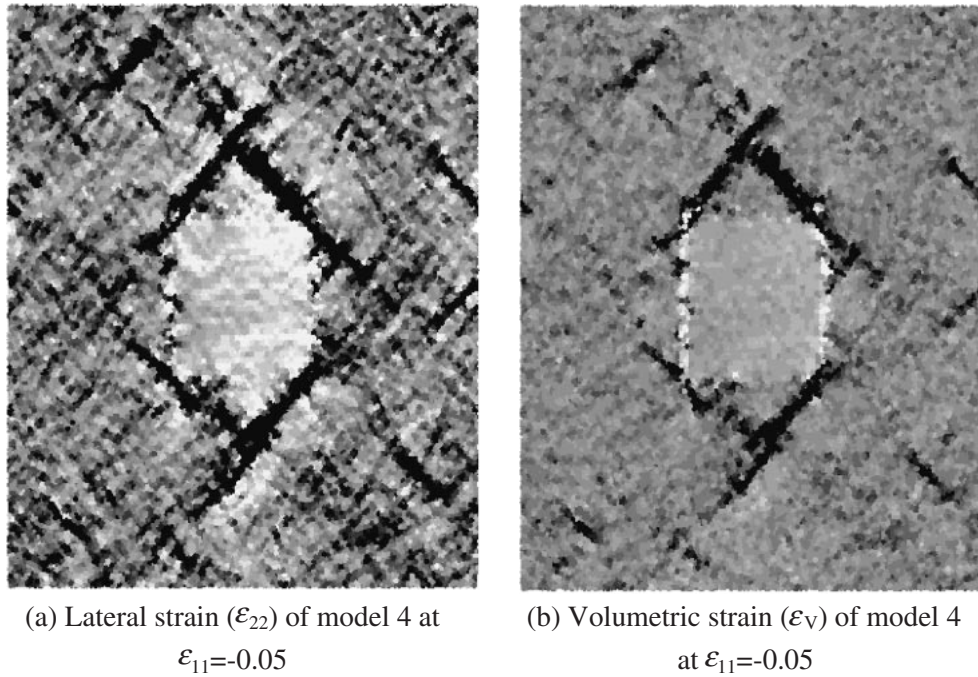


Fig. 8 (a) Contour plot of the lateral strain (ϵ_{22}) represented by colored atoms at the elastic limit ($\epsilon_{11} = -0.05$). Black represents lateral strain values larger than 0.1 while white represents 0.0 strain. (b) Contour plot of volumetric strain (ϵ_V) represented by colored atoms at the elastic limit ($\epsilon_{11} = -0.05$). Black represents a lateral strain larger than 0.1 while white represents -0.1 strain.

than the others. Consequently, in the cases of model 4 and 5, the maximum stress drops but the DPR still has a low value, indicating localized shear strain. In contrast, model 6 blocks the strain localization successfully since it has more shear bands than the other models (refer to Figs. 6 and 7).

In Figs. 6 and 7, the presence of shear bands is represented by the atomic deviatoric shear strain. Each atom is colored by the value of this strain, with black representing strains larger than 1.0, and white represents 0.0 strains. Figure 6 represents contour plots of the deviatoric atomic shear strain under tensile tests. The strain contours of each model from left to right correspond to $\epsilon_{11} = 0.05, 0.10, 0.15$ and 0.20 along the tensile direction, respectively. All models containing embedded nanocrystals except model 6 have developed coalescent voids during deformation. The voids are always generated on a shear band and/or at the interface between crystals and amorphous material, as has been seen in previous experiments.^{7,12} For values of $\epsilon_{11} = 0.1$ for each model, the onset of shear band formation corresponds well to the locations of crystals, the center of each sample. The models that develop coalescent void show relatively small number of shear bands compared to other models. This indicates that the void localizes deviatoric shear strain concentrated on the existing shear band. However, in cases where there are no voids, some shear bands prevent other shear bands propagating. Because of this behavior, the DPRs of models 1 and 6 in the tensile tests are greater than the others. The strain states, roughly corresponding to $\epsilon_{11} = 0.1$ and the maximum value of stress, indicate the onset of shear band formation. As the number of crystals is increased, the number of onset points is also roughly increased. It seems that the number of onset point is inversely proportional to the maximum stress as seen in the stress-strain curves.

Figure 7 presents contour plots of the deviatoric atomic

shear strain under compression. The strain contours of each model from left to right are corresponding to $\epsilon_{11} = -0.05, -0.10, -0.15$ and -0.20 , respectively. As seen in the experimental studies, there are no voids under the compressive loading.^{7,12} And, there are more shear bands in the compression tests compared with the tension tests. In the experiments, the number of shear bands in compression is much greater than those formed under tension.⁷ All models except model 6 shows clear and relatively long shear bands. However, for model 6, the propagation of a developed shear band is prevented by the undeveloped shear band (colored dark gray in the figure) and the presence of some tiny crystals. This means that these shear bands cannot become fully developed. We can say then, that these shear bands hinder, deflect, and bifurcate during deformation. As in the tensile tests, the onset of shear band formation ($\epsilon_{11} = 0.1$) roughly corresponds to the drop in stress.

It is noteworthy that shear bands formed in compression are accompanied by volume expansion, *i.e.* positive volumetric strain. For example, model 4 at $\epsilon_{11} = -0.05$ shows shear bands that can be clearly seen in the contour plot of lateral strain (ϵ_{22}) shown as Fig. 8(a). The region with black-colored atoms in Fig. 8(a) corresponds to the region of Fig. 8(b) where positive volumetric strain is also present. Thus, shear bands are located in regions where the volume has expanded, even under compressive loading. Consequently, even in compression, the driving force for shear band formation is the occurrence of enough volumetric expansion or enough free volume provided by the compressive loading. The free volume may originate in the inhomogeneity between amorphous and crystalline materials. The crystal structures in both Figs. 8(a) and (b) show a little less strain than at the other areas, from the observation that might provide some proof of the inhomogeneity of the materials.

4. Conclusions

We have performed 2-D molecular dynamics simulations for binary amorphous materials with embedded nanocrystals. In the simulation, the size of crystals has no significant effects for shear band formation. To the contrary, the number of nanocrystals affects the stress-strain curve and shear band formation. In particular, as the number of crystals in the materials increases, the maximum stress during deformation process decreases. The presence of many crystals in the amorphous material served as a source of shear bands. In agreement with related experimental work published so far, coalescent voids are found in the shear bands or at the interface between crystalline and amorphous materials. We also found the shear band formation started from a region with an enough free volume, even under compressive loading.

Acknowledgement

We gratefully acknowledge support from the Ministry of Education, Culture, Sports, Science and Technology in Japan, Grant-in-Aid for Scientific Research on Priority Areas (15074214).

REFERENCES

- 1) W. Klement, R. H. Wilens and P. Duwez: *Nature* **187** (1960) 869–870.
- 2) W. L. Johnson: *MRS Bull* **24** (1999) 42–56.
- 3) C. A. Pampillo: *J. Mater. Sci.* **10** (1975) 1194–1227.
- 4) F. Spapen: *Acta Metall.* **25** (1977) 407–415.
- 5) H. J. Leamy, H. S. Chen and T. T. Wang: *Met. Trans.* **3** (1972) 699–708.
- 6) J. J. Lewandowski and A. L. Greer: *Nature* **5** (2006) 15–18.
- 7) C. C. Hays, C. P. Kim and W. L. Johnson: *Phys. Rev. Lett.* **84** (2000) 2901.
- 8) C. Fan and A. Inoue: *Appl. Phys. Lett.* **77** (2000) 46–48.
- 9) K. F. Yao, F. Ruan, Y. Q. Yang and N. Chen: *Appl. Phys. Lett.* **88** (2006) 122106-1–3.
- 10) H. Kato, T. Hirano, A. Matsuo, Y. Kawamura and A. Inoue: *Scripta Mater.* **43** (2000) 503–507.
- 11) J. Lee, Y. Kim, J. Ahn, H. Kim, S. Lee and B. Lee: *Acta Mater.* **52** (2004) 1525–1533.
- 12) W. H. Jiang and M. Atzmon: *Scripta Mater.* **54** (2006) 333–336.
- 13) Y. Shi and M. Falk: *Appl. Phys. Lett.* **86** (2005) 011914-1–3.
- 14) Y. Shi and M. Falk: *Phys. Rev. Lett.* **95** (2005) 095502-1–4.
- 15) Y. Shi and M. Falk: *Phys. Rev. B* **73** (2006) 214201-1–10.
- 16) M. J. Demkowicz and A. S. Argon: *Phys. Rev. B* **72** (2005) 245205-1–16.
- 17) M. Wakeda, Y. Shibutani, S. Ogata and J. Park: *Intermetallics* **15** (2007) 139–144.
- 18) S. Kobayashi, K. Maeda and S. Takeuchi: *J. Phys. Soc. Japan* **48** (1980) 1147–1152.
- 19) S. Kobayashi, K. Maeda and S. Takeuchi: *Acta Metall.* **28** (1980) 1641–1652.
- 20) J. Park, Y. Shibutani, S. Ogata and M. Wakeda: *Mater. Trans.* **46** (2005) 2848–2855.
- 21) T. Nagase and Y. Umakoshi: *Scripta Mater.* **48** (2003) 1237–1242.
- 22) P. H. Mott, A. S. Argon and U. W. Suter: *J. Comput. Phys.* **101** (1992) 140–150.